Mol Neurobiol (2018) 55:5425–5438
DOI 10.1007/s12035-017-0776-z

Clinacanthus nutans Mitigates Neuronal Apoptosis and Ischemic Brain Damage Through Augmenting the C/EBPβ-Driven PPAR-γ Transcription

Jui-Sheng Wu[1] · Mei-Han Kao[1] · Hsin-Da Tsai[1] · Wai-Mui Cheung[1] · Jin-Jer Chen[1] · Wei-Yi Ong[2] · Grace Y. Sun[3] · Teng-Nan Lin[1,4]

Received: 28 June 2017 / Accepted: 15 September 2017 / Published online: 23 September 2017

Abstract *Clinacanthus nutans* Lindau (*C. nutans*) is a traditional herbal medicine widely used in Asian countries for treating a number of remedies including snake and insect bites, skin rashes, viral infections, and cancer. However, the underlying molecular mechanisms for its action and whether *C. nutans* can offer protection on stroke damage in brain remain largely unknown. In the present study, we demonstrated protective effects of *C. nutans* extract to ameliorate neuronal apoptotic death in the oxygen-glucose deprivation model and to reduce infarction and mitigate functional deficits in the middle cerebral artery occlusion model, either administered before or after hypoxic/ischemic insult. Using pharmacological antagonist and siRNA knockdown approaches, we demonstrated ability for *C. nutans* extract to protect neurons and ameliorate ischemic injury through promoting the anti-apoptotic activity of peroxisome proliferator-activated receptor-gamma (PPAR-γ), a stress-induced transcription factor. Reporter and chromatin immunoprecipitation promoter analysis further revealed *C. nutans* extract to selectively increase CCAAT/enhancer binding protein (C/EBP)β binding to specific C/EBP binding site (-332~-325) on the PPAR-γ promoter to augment its transcription. In summary, we report a novel transcriptional activation involving C/EBPβ upregulation of PPAR-γ expression to suppress ischemic neuronal apoptosis and brain infarct. Recognition of *C. nutans* to enhance the C/EBPβ → PPAR-γ neuroprotective signaling pathway paves a new way for future drug development for prevention and treatment of ischemic stroke and other neurodegenerative diseases.

Keywords Ischemic stroke · Gene regulation · Medicinal plant · Apoptosis

Abbreviations

ACO	Acyl-CoA oxidase
C. nutans	*Clinacanthus nutans* Lindau
CN	80% ethanol leaf extract of *C. nutans*
CNS	Central nervous system
C/EBP	CCAAT/enhancer-binding protein
ChIP	Chromatin immunoprecipitation
DMSO	Dimethyl sulfoxide
β-Gal	β-Galactosidase
icv	Intracerebroventricular
i.p.	Intraperitoneal
MCA	Middle cerebral artery
MRI	Magnetic resonance imaging
OGD	Oxygen-glucose deprivation
PNs	Primary cortical neurons
PPAR-γ	Peroxisome proliferator-activated receptor-gamma
PPRE	PPAR response element
tPA	Tissue-type plasminogen activator

✉ Teng-Nan Lin
bmltn@ibms.sinica.edu.tw

[1] Institute of Biomedical Sciences, Academia Sinica, Taipei 11529, Taiwan, Republic of China

[2] Department of Anatomy, National University of Singapore, Singapore, Singapore

[3] Department of Biochemistry, University of Missouri, Columbia, MO, USA

[4] Graduate Institute of Life Sciences, National Defense Medical Center, Taipei, Republic of China

Introduction

Stroke (or cerebrovascular disease, CVD) is the second cause of death and a leading cause of adult disability worldwide, and more than 6 million people die each year (WHO; [1]). Translation of experimental data into clinical therapy has been disappointing. Currently, tissue-type plasminogen activator (tPA) is the only FDA-approved thrombolysis treatment for acute ischemic stroke. Unfortunately, tPA has a short therapeutic window of 3~4.5 h, and less than 3~5% of stroke patients could be considered for this treatment. Although tPA has a modest efficacy in improving functional outcome, this drug is associated with a 10-fold risk of causing symptomatic intracranial hemorrhage [2–4]. Noteworthily, large population-based epidemiological and clinical studies have revealed an inverse correlation between incidents of CVD and the intake of vegetables, fruits, and herbs, in particular, plants that contain high levels of phytochemicals, such as flavonoids and sulfur compounds. There is evidence suggesting phytochemicals that exhibit anti-inflammatory and anti-oxidative properties to offer benefits to brain health [5–9].

Clinacanthus nutans Lindau (*C. nutans*) is a traditional herb grown in many tropical Asian countries and is widely used for treating snake and insect bites, skin rashes, viral infections, and more recently for treating cancer, due largely to its anti-inflammatory, anti-microbial, anti-oxidative, and anti-tumorigenic properties. However, the underlying molecular mechanisms for its mode of action remain largely unknown [10, 11]. In addition, albeit several phytochemicals, such as flavonoids and glycosides, have been documented in this medicinal plant, whether *C. nutans* also useful for treating ischemic brain injury is not known [10–12].

Recently, we reported the ability of *C. nutans* extract to protect primary cortical neurons from hypoxia-induced death through regulating histone deacetylases (HDACs) and histone acetyl transferases (HATs) [13, 14]. There is evidence that these epigenetic modifiers can exert influence on several cellular and molecular pathways involved in ischemic stroke, such as peroxisome proliferator-activated receptor-gamma (PPAR-γ) signaling [15, 16]. In the present study, we further demonstrated the ability of *C. nutans* extract to ameliorate ischemic neuronal death and brain injury via enhancing the C/EBPβ → PPAR-γ → 14-3-3ε anti-apoptotic signaling pathway.

Material and Methods

Plant Materials and Plant Extract

C. nutans leaf was originally provided by James Hung from Wincap (Malaysia). The 80% ethanol leaf extract of *C. nutans* (CN) was subsequently provided by Wei-Yi Ong (National University of Singapore) and was prepared as described previously [13, 14]. In brief, the leaves (778 g) were rinsed with distilled water and soaked in 80% ethanol (2 L) for 1 h. The leaves were blended using a homogenizer (Wiggen Hauser D-500) and the mixture was left to stand for 1 h. The ethanol extract was then filtered under vacuum (Gast USA DOA-PIO4-BN) using 90-mm glass microfiber filter membranes (Whatman, Little Chalfont, Buckinghamshire, UK). The filtrate was concentrated in a rotary evaporator at 50 °C (Buchi Labortechnik AG, Postfach, Switzerland). The resulted dark green condensate was subjected to freeze-drying (Christ Gamma 1-16 LSC) for 1–2 days. After drying, the dark green powder (27.02 g) was stored at -80 °C. The extract yield (*w*/*w*) from 778 g of fresh CN leaves was approximately 3.5%. Prior to usage, the powder extract was dissolved in dimethyl sulfoxide (DMSO), at the final concentrations of less than 0.1% and showed no toxic effect on the primary cortical neurons.

Primary Neuronal Cultures and Oxygen-Glucose Deprivation Treatment

Primary cortical neurons (PNs) preparation and oxygen–glucose deprivation (OGD) treatment were as described previously [17, 18]. In brief, PNs were prepared from E15.5 Balb/c mouse embryos and cultured in neurobasal plus B27 medium (Gibco, Grand Island, NY) containing 2 mM L-glutamine, 10 μM glutamate, 1.6% FBS, 0.4% HS, and penicillin/streptomycin. On days-in-vitro (DIV) 3, the cells were treated with 1 μM cytosine arabinoside (Ara-C) for 72 h to prevent glial proliferation and then maintained in serum-free neurobasal plus B27 medium at 37 °C in a humidified 5% CO_2 incubator. Experiments were conducted on DIV 8~14. CN and GW9662 (PPAR-γ antagonist; Cayman, Ann Arbor, MI, USA) were added to cells either at 1 h prior to, at the onset of, or immediately after OGD-treatment. In brief, OGD was conducted in a temperature-controlled (37 ± 1 °C) anaerobic chamber (Model 1025, Forma Scientific, Marietta, OH, USA) containing a gas mixture of 5% CO_2, 10% H_2, 85% N_2, and 0.02 to 0.1% O_2. Primary neurons on DIV 10 or cells grown to 70% confluence were washed with deoxygenated glucose-free Hanks' balanced salt solution (HBSS, GIBCO-BRL), and then transferred to an anaerobic chamber for 30 min. After OGD treatment, cells underwent re-oxygenation by adding equal volume of oxygenated glucose-containing HBSS and returned to the normoxic 5% CO_2/95% air incubator for various times. All chemicals were dissolved in DMSO (final concentration ≤ 0.1%). Cell viability was determined by using the cell counting kit 8 (CCK-8) (Dojindo Molecular Technologies, Kumamoto, Japan).

Flow Cytometry

Flow cytometry was employed to analyze normal mitochondria membrane potential (MMP) and apoptotic cell (sub-G_0/G_1) population [19]. For measurement of MMP, cells were stained with the fluorescent dye JC-1 (Molecular Probes, Eugene, OR), which exhibits potential-dependent accumulation in mitochondria. At low membrane potentials, JC-1 exists as a monomer and produces a green fluorescence (emission at 527 nm). At high membrane potentials, JC-1 forms J aggregates (emission at 590 nm) and produces a red fluorescence. Briefly, 1×10^6 cells were harvested and incubated with 1 ml of JC-1 in PBS (5 μg/ml) for 15 min at 37 °C in the dark. After centrifugation (500*g*, 5 min), cells were resuspended in 0.5 ml PBS and analyzed by a fluorescence-activated-cell sorter (FACS) caliber flow cytometer (BD Bioscience, San Jose, CA). For apoptosis analysis, cells were fixed in ice-cold 70% ethanol for 30 min at 4 °C. After centrifugation, cells were resuspended and incubated in phosphate-buffered saline containing 75 μg/ml RNase A and 10 μg/ml propidium iodide (PI) at 37 °C for 30 min and analyzed by FACSCalibur flow cytometer. Percent of cells with hypodiploid DNA (sub-G_0/G_1) were measured.

Western Blot Analysis

Western blot analysis of protein levels in primary neurons and brains were performed as described previously [18] with antibodies from Santa Cruz Biotechnology (Santa Cruz, CA, USA): PPAR-γ (1:500), 14-3-3ε (1:500), α-tubulin (1:1000); Cell Signaling Technology (Danvers, MA, USA): p-Bad (1:250), Bad (1:500), cleaved caspase-3 (Caspase3; 1:500), cleaved poly(ADP-ribose) polymerase 1 (PARP; 1:1000); BD Bioscience (San Jose, CA, USA): Bcl-2 (1:500); GeneTex Inc. (San Antonio, TX, USA): GFP (1:1000). Protein bands were visualized by enhanced chemiluminescence system (Merck Millipore; Billerica, MA, USA).

Small Interference RNA Transient Transfection

Specific small interference RNA (siRNA) and scramble RNA (scRNA, control) were purchased from Ambion (Austin, TX, USA; PPAR-γ—80 nmol/L); Santa Cruz (C/EBPα, β and δ—40 nmol/L) and MDBio (Taipei, Taiwan-ROC; scRNA). mRNA-In® Neuro (MTI-GlobalStem, Gaithersburg, MD, USA) was used as transfection carrier. In brief, 1.5 μl of mRNA-In® Neuro and siRNA were mixed with 50 μl of Optimedium and then added into 24-well dish containing 2.5×10^5 primary neurons/well. At 5 h after transfection, the medium was replaced by culture medium containing neurobasal plus B27 medium and cultured for another 19 h before OGD treatment. Transfection efficiency (~ 70%) was evaluated by transfecting FAM-labeled siRNA (MDBio), and enhanced green fluorescent protein in primary neurons was measured by flow cytometry and fluorescence microscopy. [20]

RNA Isolation, Reverse Transcription and Polymerase Chain Reaction

Total RNA of PNs and cortex were isolated by Direct-zol RNA MiniPrep (Zymo Research, CA, USA) per manufacturer's instructions as described previously [18, 21]. RT was performed by SensiFAST cDNA synthesis kit (Bioline, London, UK) per manufacturer's instruction. PCR amplification was carried out by incubating 1~2 μl RT reaction product with KAPA2G Fast HotStart ReadyMix PCR kit (KAPABIOSYSTEMS, Boston, USA) for 25~30 cycles at annealing temperature (T_{ann}). Mouse primer sequences and T_{ann} were listed in Table 1.

Transient Transfection and Reporter Assay

PPRE-containing acyl-CoA oxidase (ACO) and 14-3-3ε reporter constructs were prepared by cloning a mouse promoter sequence into the pGL4-Luc vector (Promega, Madison, WI, USA) as previously described [22, 23].

For cloning PPAR-γ (H) and C/EBP (m) promoters, 5′-flanking region of human or mouse genomic sequence, respectively, was synthesized by the primer sequences listed in Table 2.

PCR products were cloned into pGL4 luciferase reporter. A minimal cytomegalovirus promoter pCMV-β-galactosidase (β-Gal) plasmid (Promega) was used as an internal control of transfection. Cells were lysed with Reporter Lysis Buffer (Promega) and the luciferase activity was then determined by mixing 50 μl of the cell lysate with 50 μl of the Luciferase Assay Reagent.

Transfection protocol for mouse PNs was adopted from N2A neuroblastoma cells as previously described with modifications [18]. In brief, 1.25 μl of DNA-In® Neuro (MTI-GlobalStem) and 0.5 μg of DNA were mixed with 30 μl of Optimedium then added into 24-well dish containing 2.7×10^5 neuronal cells/well. Three hours after transfection, 0.5 ml medium was added to each well and incubated for another 21 h prior to OGD treatment. Transfection efficiency (~ 25%) was evaluated by transfection of pEGFP-N1, and measurement of enhanced green fluorescent protein in cells using flow cytometry, reporter activity, fluorescence microscopy, and Western blot.

Chromatin Immunoprecipitation Assay

Chromatin immunoprecipitation (ChIP) assay was performed as described [22, 23]. In brief, 5×10^6 primary neurons were incubated in 1% formaldehyde for 15 min at RT. Glycine

Table 1 Oligonucleotide sequence of amplification primers for PCR

Gene	Primer sequence (5′-3′)	T_{ann} (°C)
PPAR-γ	F:ATG,GTT,GAC,ACAGAG,ATG,CCA,TTC	57
	R:GTG,GAT,CCG,GCA,GTT,AAG,ATC,ACA,CC	
β-actin	F:CAT,CCG,TAA,AGA,CCT,CTA,TGC,CAA,C	57
	R:CAA,AGA,AAG,GGT,GTA,AAA,CGC,AGC	
14-3-3ε	F:ATG,GAT,GAT,CGG,GAG,GAT,CTG	57
	R:GTC,CAG,TAC,ATC,CAG,AAT,GTC,AC	
C/EBP	F:CGG,CGS,GAR,CGC,AAC,AA	61
	R:GGG,CAG,RTM,BYK,GAA,SAW,SYB,CCG,SAG	
C/EBPα	F:GTG,GAC,AAG,AAC,AGC,AAC,GA	61
	R:TCA,CGC,GCA,GTT,GCC,CA	
C/EBPβ	F:TTC,ATG,CAC,CGC,CTG,CTG	60
	R:CGG,CTT,CTT,GCT,CGG,CTT	
C/EBPδ	F:ATG,AGC,GCC,GCG,CTT,TT	61
	R:CGC,TTT,GTG,GTT,GCT,GTT,GAA	
STAT5b	F:CAT,GGC,TAT,GTG,GAT,ACA,GGC,T	57
	R:GGC,CTT,AAT,GTT,CTC,CTG,TGG,A	
STAT1	F:TAC,AGC,CGC,TTT,TCT,CTG,GAG	57
	R:CCC,TCC,TGG,GCC,TGA,TTA,AAT	
NFATC2	F:TGG,CCC,GCC,ACA,TCT,ACC,CT	57
	R:TGG,TAG,AAG,GCG,TGC,GGC,TT	
NFATC4	F:ACA,TTG,AGC,TAC,GGA,AGG,GTG,AGA	57
	R:ACT,CGA,TGG,GCA,CTG,ATG,CT	

(0.125 M) was added for another 5 min. Cells were washed twice with ice-cold PBS, scraped, and lysed in lysis buffer (50 mM HEPES, pH 7.5, 140 mM NaCl, 1% triton X100, 0.1% Na-deoxycholate with 1× Thermo-Halt protease inhibitor) for 10 min at 4 °C. Lysates were sonicated 24 times at amplitude 50 and centrifuged at 16,200*g* for 10 min at 4 °C to remove debris. An amount of 300 μg lysate of protein was used as DNA input control or incubated with various antibodies against C/EBPα, C/EBPβ, C/EBPδ (GeneTex Inc.); or non-immune rabbit IgG at 4 °C overnight. Immunoprecipitated complexes were collected by using protein G-Sepharose beads. The precipitates were extensively washed and incubated in the elution buffer (1% SDS, 10 mM EDTA, and 50 mM Tris, pH 8.0) for 10 min at 65 °C. Cross-linking of protein−DNA complexes was reversed at 65 °C for 6 h to overnight, followed by treatment with 100 μg/ml proteinase K for 3 h at 50 °C. DNA was extracted by use of a PCR purification kit (Qiagen, Duesseldorf, Germany), then underwent PCR amplification with the primers for (1) C/EBP-A site (-550~-410), F: 5′-tcagaaacactgctaagaaatttaag-3′, R: 5′-cagagttccttgcgtttgtaagtt-3′; (2) C/EBP-B site (-400~-260), F: 5′-ttaaattttcttttaaaatgtcactgga-3′, R: 5′-atgcccccggccaggg-3′; (3) C/EBP-C site (-250~-110), F: 5′-ttcggatccctcctcgga-3′, R: 5′-agtagggcccacggcgg-3′. Putative C/EBP binding sites (T00017) with typical TTGC.CAACTC motif on mouse PPAR-γ1 promoter region were analyzed with "ALGGEN-Promo" (see http://alggen.lsi.upc.es/cgi-bin/promo_v3/promo/promoinit.cgi?dirDB=TF_8.3.).

Middle Cerebral Artery Occlusion Stroke Model

The focal cerebral ischemia model entailing 3-vessel occlusion was as reported [24]. In brief, 7 to 8 week-old male Long-Evans rats purchased from The National Laboratory Animal Center (NLAC; Taipei, Taiwan) were anesthetized with chloral hydrate (360 mg/kg body wt, i.p.). The right middle cerebral artery (MCA) was ligated reversibly with a 10-0 suture and both common carotid arteries (CCAs) were also occluded reversibly with aneurysm clips. Triple vessel occlusion was held for 30 min and then the suture and the aneurysm clips were released with restoration of blood flow in the three arteries verified. Animals were kept in an air-ventilated incubator at 26.0 ± 0.5 °C and sacrificed under anesthesia at variable time intervals after ischemia. Brains were removed and the ischemic and contralateral cerebral cortices were dissected and frozen. Infarct area was delineated by 2,3,5-triphenyltetrazolium chloride (TTC) and infarct volume was measured as previously described [24]. Animals subjected to vascular surgeries but without right MCA and bilateral CCA occlusion served as sham-operated controls. Arterial blood gases and mean arterial pressure were also monitored in selected animals at 30 min before, during, and after ischemia. The values were within normal range before, during, and after ischemia. All procedures were performed in accordance with the Public Health Service Guide Approved Procedures for the Care and Use of Laboratory Animals and approved by the Academia Sinica Animal Studies Committee (IACUC, http://iacuc.sinica.edu.tw/). CN and siRNA treatments were performed in random order, by an investigator blinded to the surgical groups.

Intracerebroventricular Infusion and Intraperitoneal Injection

The intracerebroventricular (icv) infusion procedure was performed as previously described [22, 25]. Briefly, anesthetized rats were placed in a stereotaxic apparatus; 10 μl of artificial cerebrospinal fluid (aCSF) with chemicals was infused into the right lateral ventricle at a rate of 2 μl/min at the following coordinates: anterior, 2.5 mm caudal to bregma; right, 2.8 mm lateral to midline; and ventral, 3.0 mm ventral to dural surface. Rats were infused with CN extract (10~60 pg), GW9662 (165 ng), PPAR-γ or C/EBPβ siRNA (0.5 nmol) immediately after a 30-min MCA occlusion. Periodic confirmation of proper placement of the needle was performed with infusion of fast green. On the other hand, rats were subjected to intraperitoneal (i.p.) injection of CN extract (24 mg/kg body wt) at 1 h prior to

Table 2 Primers for promoter cloning

Reporter gene	Primer sequence (5′-3′)
PPAR-γ (H)	
p1000-Luc (-1000 to 1)	F: TTT,GGT,ACC,AAG,CGC,TGA,ATA,TTT,TCC,CTT,GT
	R:TTT,CTC,GAG,CGC,CGG,CTG,GGG,GTG,GGG,GT
p500-Luc (-500 to 1)	F:TTT,GGT,ACC,CAG,TGA,CTT,GTG,AAT,AAC,CAT,GTA,ACT,TAC
	R:TTT,CTC,GAG,CGC,CGG,CTG,GGG,GTG,GGG,GT
p441-Luc (-441 to 1)	F:TTT,GGT,ACC,GAT,CAG,AAG,AGA,AAA,CCA,AGG,GAC,C
	R:TTT,CTC,GAG,CGC,CGG,CTG,GGG,GTG,GGG,GT
p319-Luc (-319 to 1)	F:TTT,GGT,ACC,CTG,GCC,GAG,AGG,GAG,CCC,CAC,A
	R:TTT,CTC,GAG,CGC,CGG,CTG,GGG,GTG,GGG,GT
p258-Luc (-258 to 1)	F:TTT,GGT,ACC,CTA,AAC,TTC,GGA,TCC,CTC,CTC
	R:TTT,CTC,GAG,CGC,CGG,CTG,GGG,GTG,GGG,GT
p150-Luc (-150 to 1)	F:TTT,GGT,ACC,GAG,AGT,GGA,CGC,GGG,AAA,G
	R:TTT,CTC,GAG,CGC,CGG,CTG,GGG,GTG,GGG,GT
Nested primers	
DA-p1000-Luc (-475~-468 deletion)	F1:ACC,ATG,TAA,CTT,ACG,GAA,CTC,TGA,AAG,T
	R1:ACT,TTC,AGA,GTT,CCG,TAA,GTT,ACA,TGG,T
DB-p1000-Luc (-332~-325 deletion)	F1: CCG,ATC,GCC,GTG,TGG,CCA,CTC,TGG,CCG,A
	R1: TCG,GCC,AGA,GTG,GCC,ACA,CGG,CGA,TCG,G
DC-p1000-Luc (-192~-185 deletion)	F1: CAG,CGG,TGG,TGG,CGA,CGA,CAC,CAG,GTA,G
	R1: CTA,CCT,GGT,GTC,GTC,GCC,ACC,ACC,GCT,G
C/EBPα (m)	
p1000-Luc (−1000 to 1)	F: TTT,GGT,ACC,TCC,CCG,ATT,CAA,GTT,CAC,TCC
	R: TTT,CTC,GAG,TTC,GGG,TCG,CGA,ATG,GC
C/EBPβ (m)	
p1000-Luc (-1000 to 1)	F: TTT,GGT,ACC,GTC,AAT,GGG,TCG,GGG,GTC,A
	R: TTT,CTC,GAG,AAC,GGG,CTG,CGT,CAC,GCT
C/EBPδ (m)	
p1000-Luc (-1000 to 1)	F: TTT,GGT,ACC,GGA,GCT,AGG,CTG,CTC,TGT,GTA,AAT
	R: TTT,AAG,CTT,TGT,CAC,CTC,GCC,GGG,C

or 3~24 h after a 30-min MCA occlusion; or at 1 day after a 15-min MCA occlusion. Infarct volume was assessed at 1-day or 2-day reperfusion, respectively.

Behavioral Assessments

Mice after MCA occlusion exhibited unilateral forelimb weakness and flexion with reduced resistance when suspended by tail and applied pressure on their shoulders. *Bederson's test* was used to evaluate neurological deficits based on these postural reflexes before MCA occlusion and 7 and 14 days after MCA occlusion by investigators blinded to the study conditions. Rats were scored based on the following criteria: grade 5 (normal); grade 4 (forelimb flexion and no other abnormalities); grade 3 (reduced resistance to lateral push toward the paretic side, and forelimb flexion); grade 2 (same behavior as grade 3, with circling toward the paretic side when pulling the tail on the table); grade 1 (same behavior as grade 2, with spontaneous circling); grade 0, no activity [18, 26]. *Elevated body swing test*: Animals were examined for asymmetrical motor behavior using the elevated body swing test at before MCA occlusion and 7 and 14 days after MCA occlusion by investigators blinded to the study conditions. Animals were held by the tail and elevated about an inch from the bottom of a Plexiglas box. During 20 trials, the direction and number of times that the animal moved more than 10° to either the left or right side of the vertical axis were recorded. Each animal had to return to the vertical position before the next swing was counted. Intact animals do not exhibit a uniform side biased swing although individual animals may exhibit a preferential side biased swing [18, 27]. *Ladder rung walking test:* The ladder rung walking task, used to determine loss and recovery of sensorimotor functions, was performed as described [28]. Rats were trained (two trials per day) for 3 days to cross a 1.8-m-long horizontal ladder rung walking task with regular spaced round metal rungs (3.0 mm

diameter/1.5 cm apart) before baseline evaluation. At 14 days after stroke, the rats were filmed to cross the ladder with an irregular rung random distances ranging from 1.5 to 4.5 cm in three trials. The percentage of foot errors were calculated by counting the number of slips of hindlimb and forelimb relative to the total number of steps. All experiments were performed by a trained investigator blinded to the experimental conditions.

Magnetic Resonance Imaging

MRI studies were performed on a 7-T PharmaScan 70/16 MR scanner (Bruker Biospin GmbH, Germany) with an active shielding gradient (30 G/cm in 80 μs). Rats were initially anesthetized with 5% isoflurane and maintained with 1.5 to 2.0% isoflurane at 2 L/min air flow. Rats were allowed to breathe spontaneously throughout the experiments. Rats were placed in a prone position and fitted with a custom-designed head holder inside the magnet, as previously described [29]. Images were acquired using a 72-mm birdcage transmitter coil and a separate quadratic surface coil for signal detection. Multi-slice axial FES T2WI were acquired with a field of view of 3.0 × 3.0 cm^2, a matrix size of 256 × 128 with zero-filling to 256 × 256, repetition time = 4500 ms, echo time = 70 ms, bandwidth = 50 kHz, slice thickness = 1 mm, number of averages = 8, and the total acquisition time is 9 min 36 s. T2WI was assessed by TMC core service engineers blinded to the study conditions at 7 or 14 days after ischemia.

Statistical Analysis

ANOVA was used to compare the expression of proteins, mRNA, or infarct volumes. Differences between groups were further analyzed by post hoc Fisher's protected *t* test by use of GB-STAT 5.0.4 (Dynamic Microsystems, Silver Springs, MD). $P < 0.05$ was considered significant. Studies were performed at least $n = 3$ in triplicates for in vitro studies and $n \geq 6$ for in vivo studies.

Results

A. *C. nutans* leaf extract (CN) protects mouse primary cortical neurons (PNs) against oxygen-glucose deprivation (OGD)-induced apoptotic death via a PPAR-γ-dependent pathway

To investigate the protective effects of CN, PNs were subjected to OGD up to 12 h (H0.5~H12) (Fig. 1a) or 0.5 h OGD plus reoxygenation for 4 to 24 h (H0.5R4 ~H0.5R24) (Fig. 1b). As shown in Fig. 1a, cell viability was decreased with increasing time of hypoxia; neurons subjected to 0.5 h OGD (H0.5) showed survival of 64.09 ± 1.93%, and decreased to 25.43 ± 0.23% after 12 h (H12). When PNs were pretreated with 6.25 μg/ml of CN 1 h prior to OGD, significant increase in cell viability was observed at all times of OGD (Fig. 1a). Similarly, neuronal viability was decreased with increasing time of reoxygenation; only 39.12 ± 5.26% of cells remained viable at 24 h after a 0.5 h OGD (H0.5R24). CN pretreatment significantly improved cell viability at all times after reoxygenation (Fig. 1b). We next tested the concentration of CN to ameliorate neuronal death after H0.5R24 insult. As shown in Fig. 1c, significant concentration-related protection was observed after adding 0.15 μg/ml CN at the onset of OGD. Furthermore, significant protection was observed when 6.25 μg/ml CN was applied before, at the onset, and after OGD, albeit that the effect was less when applied after onset of OGD (Fig. 1d).

We subsequently investigated possible mechanism for CN to ameliorate OGD-induced neuronal death by examining the mitochondria membrane potential (MMP) and population of sub-G0/G1 (i.e., apoptosis) in PNs by flow cytometer using JC-1 and PI staining. At normoxic control (H0), 89.18 ± 2.71% PNs exhibit normal MMP, whereas normal MMP cells decreased to 41.71 ± 2.44% when subjected to H0.5R12 (Fig. 1e). Treatment with 6.25 μg/ml CN at the onset of OGD significantly protected PNs from MMP breakdown (62.53 ± 3.8%). Surprisingly, the protective effect of CN was abrogated by co-treatment with 10 μM GW9662 (GW), a PPAR-γ antagonist (Fig. 1e). GW9662 per se was shown not to alter cell viability [20]. Concurrently, a significant increase in apoptotic population from 7.0 ± 0.46% to 30.28 ± 5.06% was noted when PNs was subjected to H0.5R24. Treatment with CN at the onset of OGD attenuated apoptotic PNs death, and the protective effect of CN was abrogated by GW9662 (Fig. 1f).

We further analyzed effects of CN on the levels of pro-apoptotic markers, e.g., cleaved caspase-3 and PARP-1, and the anti-apoptotic markers, e.g., 14-3-3ε, p-Bad and Bcl-2 in PNs subjected to H0.5R24. As shown in Fig. 1g, cleaved caspase-3 and PARP-1 protein levels were dramatically increased after H0.5R24 and were suppressed after CN treatment. Simultaneously, there was a significant decrease in levels of 14-3-3ε, p-Bad, and Bcl-2 protein, and these changes were reversed by CN. Again, the anti-apoptotic effect of CN was counteracted by GW9662 (Fig. 1g).

The involvement of PPAR-γ in CN's neuroprotective effect was confirmed by silencing of PPAR-γ. In this study, PNs were first transfected with PPAR-γ scRNA (or siRNA) for 24 h and was followed by treatment with either DMSO Con or 6.25 μg/ml CN prior to H0.5R24; and then followed with mRNA level and apoptosis analysis. As shown in Fig. 1h, PPAR-γ siRNA transfection not only inhibited PPAR-γ mRNA expression as compared to the scRNA control (upper panel), but also abrogated the anti-apoptotic effect of CN (lower panel).

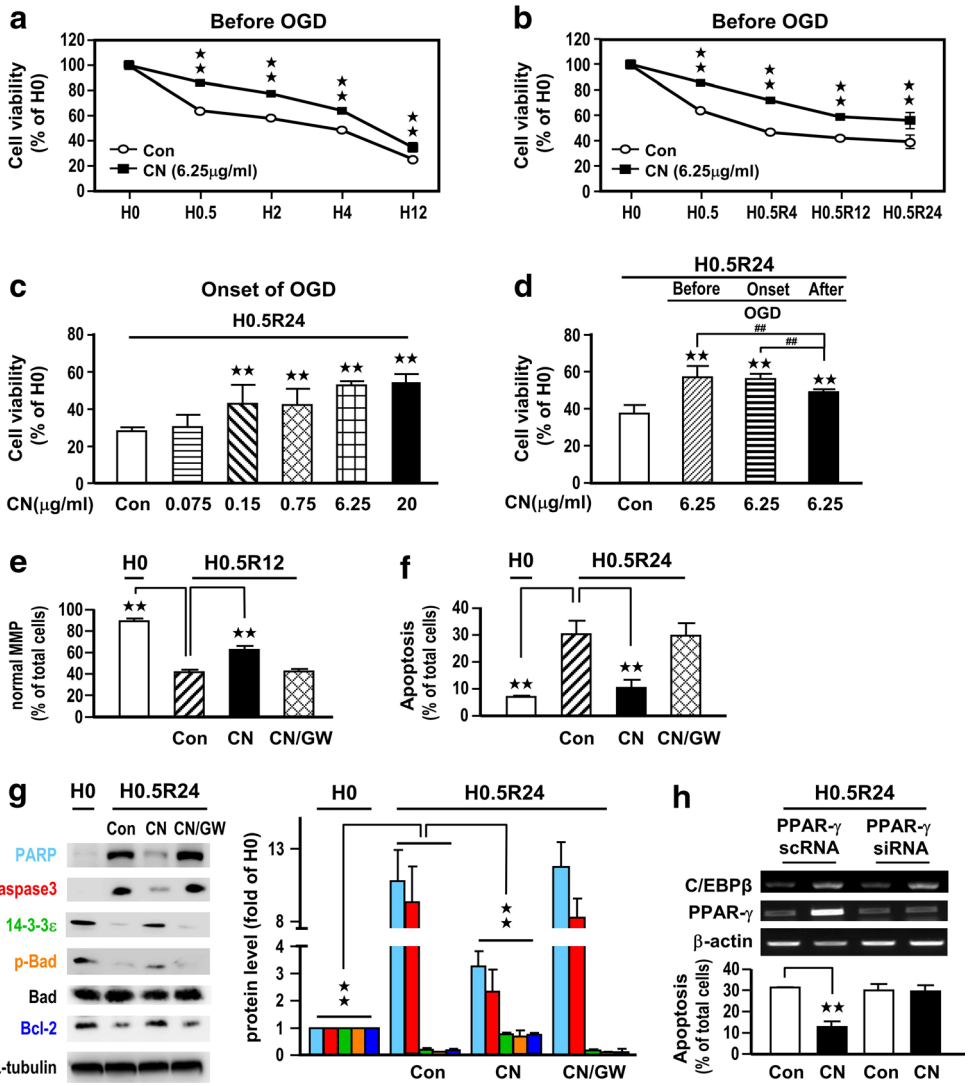

Fig. 1 *C. nutans* extract (CN) protected primary cortical neurons (PNs) from OGD-induced cell death. PNs were pretreated with CN 1 h before subjected to 0.5 to 12-h OGD (H0.5~H12; **a**) or 0.5-h OGD plus 4- to 24-h reoxygenation (H0.5R4~H0.5R24; **b**). PNs were treated with CN either at the onset of (**c**) or immediately after (**d**) OGD. PNs were treated with 6.25 μg/ml CN and 10 μM GW9662 (GW) at the onset of OGD (e~g). PNs were transfected with 80 nM PPAR-γ siRNA, then treated with 6.25 μg/ml CN at the onset of OGD (**h**). Inset shows representative protein or mRNA bands. H0 refers to no OGD control. Data are mean ± SD of at least three independent experiments performed in triplicate. $^{\star\star}P < 0.01$ versus vehicle control. $^{\#\#}P < 0.01$ between designed groups

Experiments were carried out to further investigate the relationship between CN and PPAR-γ. As shown in Fig. 2a, transient OGD (H0.5R24) resulted in a significant increase in PPAR-γ mRNA. Treatment with CN (2.5 to 10 μg/ml) at the onset of OGD led to a concentration-dependent increase in PPAR-γ mRNA levels in PNs. Furthermore, CN (6.25 μg/ml) also mediated a time-dependent increase in PPAR-γ mRNA up to H0.5R48 (Fig. 2b). Reporter assays was used to examine whether CN-induced PPAR-γ upregulation is due to transcriptional activation. PPAR-γ-p1000-Luc, ACO-$(PPRE)_4$-Luc, or 14-3-3ε-p1625-(PPRE)-Luc reporter constructs were transfected into PNs for 24 h and followed by treatment with CN for another 24 h. As shown in Fig. 2c, CN at 2.5 and 6.25 μg/ml proportionally increased PPAR-γ (p1000)-reporter activity. Furthermore, 6.25 μg/ml CN also significantly increased ACO-reporter activity, which contains four PPAR response element (PPRE) sites (Fig. 2d), and 14-3-3ε-reporter activity, which has 1-PPRE site and a known downstream gene of PPAR-γ (Fig. 2e). Assay of 14-3-3ε mRNA showed corresponding increase in expression due to CN (Fig. 2f). These results revealed that CN protected PNs by activating the anti-apoptotic PPAR-γ → 14-3-3ε pathway [22].

B. *C. nutans* leaf extract (CN) enhances C/EBPβ binding to PPAR-γ promoter and augments its transcription

To examine how CN regulates PPAR-γ transcription, PNs were transfected with six PPAR-γ reporter plasmids with serial deletion on the 5′-flanking regions of human PPAR-γ promoter for 24 h. Subsequently, the transfected cells were subjected to H0.5R24 with treatment of 6.25 μg/ml CN at the onset of OGD. As shown in Fig. 3a, the p1000-Luc reporter activity was greatly enhanced by CN at H0.5R24, but gradually declined upon shortening the 5′-flanking region of PPAR-γ promoter; while no effect was observed at p319-Luc and beyond. Since no difference in reporter activity was noted between p1000-Luc and p500-Luc, and both activities

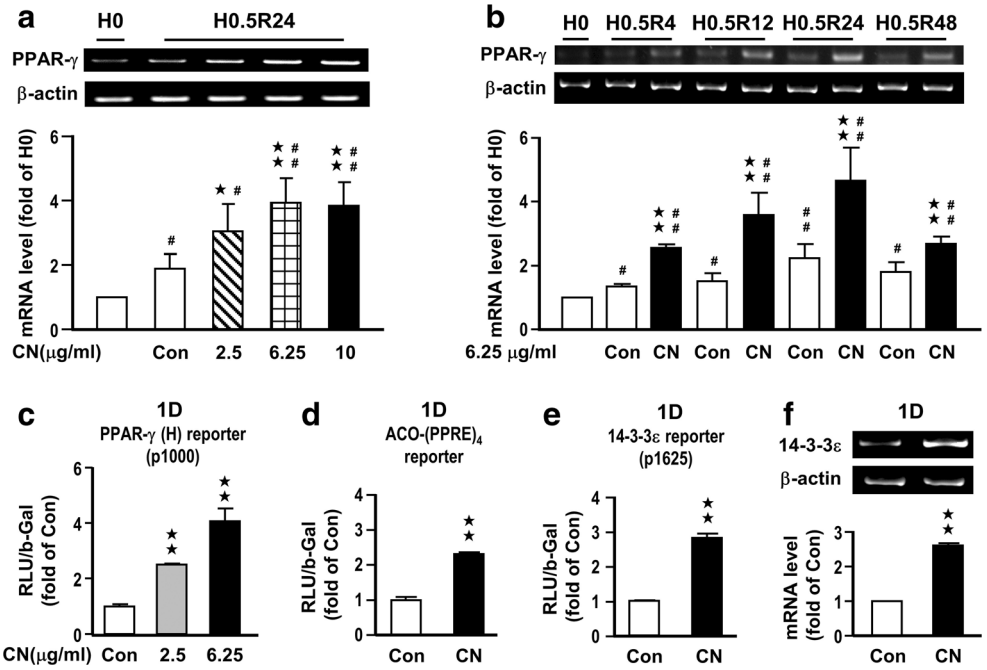

Fig. 2 *C. nutans* extract (CN) enhanced PPAR-γ transcription. PNs were treated with increasing amount of CN (**a**) or 6.25 μg/ml of CN (**b**) at the onset of OGD. PNs were transfected with 0.5 μg reporter plasmids of PPAR-γ (**c**), ACO (**d**), 14-3-3ε (**e**), or without (**f**) for 24 h, and then treated with 6.25 μg/ml CN for another 24 h (1D). Insert shows representative mRNA bands. Reporter activity is expressed as relative light units (RLU) with β-gal (b-Gal) as a normalization control. Data are mean ± SD of at least three independent experiments performed in triplicate. $^{\#}P < 0.05$ and $^{\#\#}P < 0.01$ versus H0. $^{\star}P < 0.05$ and $^{\star\star}P < 0.01$ versus vehicle control

were significantly higher than p441-Luc (Fig. 3a), we further analyzed transcription factor binding sites within the (-500~-300) 5′-flanking region of PPAR-γ with the ALGGEN-Promo search engine, which suggested C/EBP, STAT, and NFAT as potential candidates. RT-PCR results showed that upon increasing amount of CN treatment, only the levels of C/EBP mRNA were positively correlated with the expression of PPAR-γ in PNs at H0.5R24 (Fig. 3b).

Two potential C/EBP binding sites were identified within (-500~-300) 5′-franking region of PPAR-γ: (-475~-468) (A site) and (-332~-325) (B site), together with (-192~-185) (C site; additional control). To examine the importance of each site, PNs were transfected with A, B, or C site deleted p1000-Luc reporter plasmids and then treated with 6.25 μg/ml CN prior to H0.5R24. Results indicated that CN lost its reporter augmentation ability completely in PNs transfected with B site-deleted plasmid (Fig. 3c). A slight but significant decrease in reporter activity was noted with A site deletion, while no effect was observed upon deletion of C site. These results are in agreement with results observed in Fig. 3a.

We subsequently analyzed mRNA levels of C/EBPα, β, and δ isoforms and their response to CN treatment. As shown in Fig. 4a, PPAR-γ, C/EBPα, and C/EBPβ mRNAs were increased in PNs subjected to H0.5R24, whereas no change was noted in C/EBPδ mRNA level. Similar to PPAR-γ, C/EBPβ mRNA level was further augmented after treatment with increasing CN at the onset of OGD, whereas C/EBPα and C/EBPδ mRNA levels were not significantly affected by CN treatment (Fig. 4a). Reporter assays further confirmed that only PNs transfected with C/EBPβ reporter construct but not with the C/EBPα and C/EBPδ constructs showed enhanced activity by 6.25 μg/ml CN (Fig. 4b).

ChIP analysis revealed basal binding of C/EBPβ onto B site of PPAR-γ promoter at normoxia (H0). While hypoxia increased this binding, 6.25 μg/ml CN further enhanced this binding in PNs subjected to H0.5R12 (Fig. 4c). Despite that some C/EBPβ was bound to A site at H0, this binding was not influenced by OGD or CN treatment. Since deleting A site slightly and significantly reduced reporter activity (Fig. 3a, c), it is possible that this site is needed for optimal activity. No binding to C site was detected (Fig. 4c). A low level of C/EBPα was bound to C site of PPAR-γ promoter at H0, and hypoxia increased this binding. However, CN treatment did not further enhance this binding at H0.5R12 (Fig. 4c). Although a very small amount of C/EBPα bound to B site, OGD and CN treatment did not exert any effect on its binding. Meanwhile, no binding to A site was detected (Fig. 4c). Since C site deletion has no effect on PPAR-γ reporter activity (Fig. 3c), the aforementioned results confirmed that C/EBPα did not participate in the protective effect of CN. There was no binding of C/EBPδ with A, B, or C sites (Fig. 4c).

Knockdown approach was used to confirm that CN protects PNs from OGD-induced cell death through C/EBPβ → PPAR-γ signaling pathway. In this study, C/EBPβ siRNA transfection decreased not only C/EBPβ but also PPAR-γ mRNA levels as compared to the scRNA control (Fig. 4d, left), while PPAR-γ siRNA transfection did not alter C/EBPβ mRNA level (Fig. 1h, upper). Concurrently, C/EBPβ siRNA also abrogated the anti-apoptosis ability of CN (Fig. 4d, right). On the other hand, neither the PPAR-γ

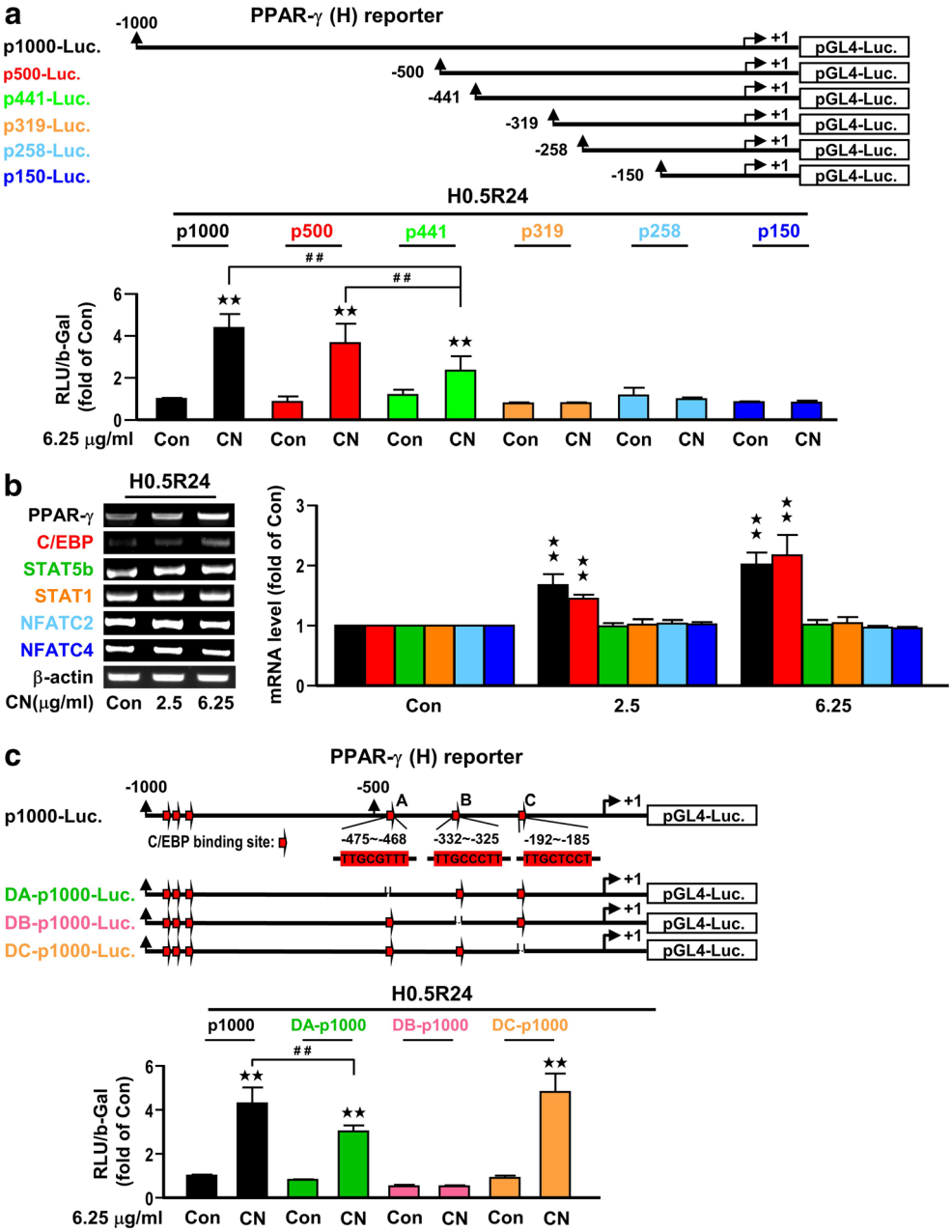

Fig. 3 PPAR-γ transcription enhanced by *C. nutans* extract (CN) was C/EBP-dependent. PNs were transfected with 0.5 μg of reporter plasmids for 24 h, and then treated with CN at the onset of OGD (**a**). PNs were treated with increasing amount of CN at the onset of OGD (**b**). PNs were transfected with 0.5 μg of reporter plasmids, and then treated with CN at the onset of OGD (**c**). Inset shows representative mRNA bands. Reporter activity is expressed as relative light units (RLU) with β-gal (b-Gal) as a normalization control. Data are mean ± SD of at least three independent experiments performed in triplicate. $^{\star\star}P < 0.01$ versus vehicle control. $^{\#\#}P < 0.01$ between designated groups

level nor the anti-apoptotic effect of CN was altered by C/EBPα or C/EBPδ siRNA (data not shown).

C. *C. nutans* leaf extract (CN) ameliorates apoptotic neuronal death, cerebral infarct, and behavioral deficits in the rat MCA occlusion model

With the above in vitro findings, an important next step is to test whether CN may inhibit ischemic brain damage in vivo. In this study, CN was administered by icv infusion immediately after 30-min MCA occlusion. Control rats were infused with same amount of aCSF but without CN. Assessment of infarct volume at 1-day reperfusion showed reduction of infarct volume by CN in a dose-dependent manner, reaching a maximal decrease at 40 pg (Fig. 5a). Furthermore, the protective effect of CN was abrogated by concomitant treatment of 165 ng of GW9662, the PPAR-γ antagonist (Fig. 5a). Concurrently, PPAR-γ, 14-3-3ε, and C/EBPβ mRNA levels were upregulated in the rat brain cortices subjected to CN treatment, whereas C/EBPα and C/EBPδ mRNA levels were not altered (Fig. 5b). Under this ischemic condition, the ability of CN to reduce infarct volume was abrogated by concomitant infusion of PPAR-γ siRNA (Fig. 5c), which effectively knocked down PPAR-γ level but leaving C/EBPβ level unaltered. Correspondingly, infusion of C/EBPβ siRNA not only knocked down C/EBPβ but also

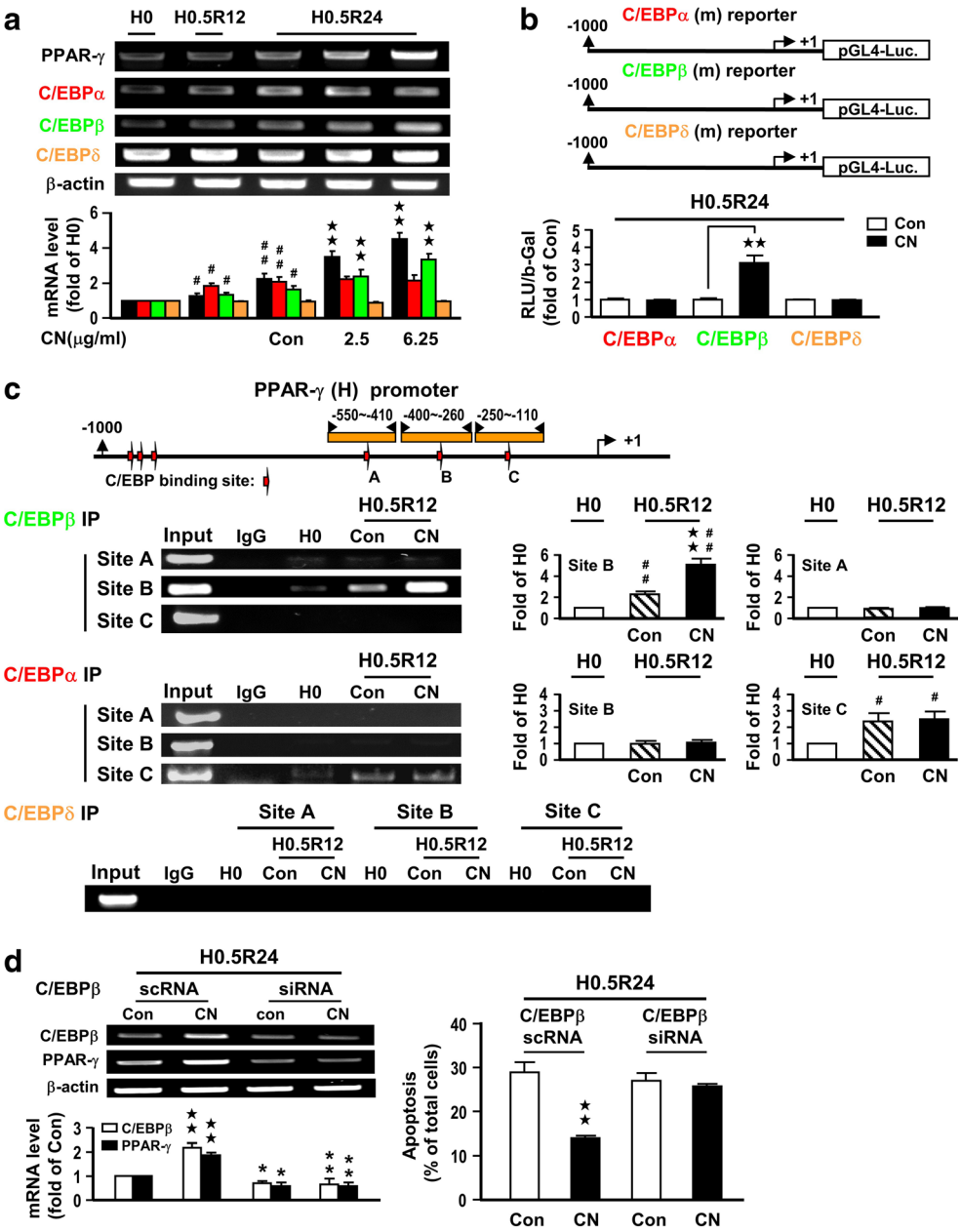

Fig. 4 *C. nutans* extract (CN) via augmenting C/EBPβ binding to site B enhanced PPAR-γ transcription. PNs were subjected to OGD-reoxygenation with CN treatment at the onset of OGD (**a**). PNs were transfected with 0.5 μg reporter plasmids, and then treated with 6.25 μg/ml CN at the onset of OGD (**b**). Binding of C/EBPs onto PPAR-γ promoter were further examined by ChIP assay (**c**). PNs were transfected with 40 nM C/EBPβ siRNA, and then treated with 6.25 μg/ml CN at the onset of OGD (**d**). Inset shows representative PCR bands. Reporter activity is expressed as relative light units (RLU) with β-gal (b-Gal) as a normalization control. Data are mean ± SD of at least three independent experiments performed in triplicate. $^{\#}P < 0.05$ and $^{\#\#}P < 0.01$ versus H0. $^{\star\star}P < 0.01$ versus vehicle control. $^{*}P < 0.05$ and $^{**}P < 0.01$ versus scRNA

PPAR-γ levels (Fig. 5c, upper panel). Both PPAR-γ siRNA and C/EBPβ siRNA treatment abrogated the ability for CN to reduce infarct volume (Fig. 5c, lower panel). These results confirmed that C/EBPβ is upstream of PPAR-γ in the in vivo model. Similar to the OGD study, pro-apoptotic cleaved PARP-1 and cleaved caspase 3 protein levels were downregulated in the CN treated group, whereas the anti-apoptotic 14-3-3ε, p-Bad, and Bcl-2 levels were upregulated (Fig. 5d). In addition, at 7 days (1 week) after ischemia, CN treatment resulted in better functional outcomes as based on elevated body swing test (Fig. 5e) and Bederson's postural reflex task (Fig. 5f). At 14 days (2 weeks) after ischemia, the CN treated group performed better at ladder rung walking test (Fig. 5g) and sustained smaller infarct volumes (Fig. 5h).

The beneficial effect of CN was also investigated in the experimental paradigm in which CN was delivered via intraperitoneal (i.p.) injection. In this study, rats were given i.p. injections of CN 24 mg/kg 1 h before 30-min MCA occlusion and followed by measurement of infarct volume at 24 h (1D) reperfusion. Under this condition, infarct volume was significantly lower in rats receiving CN than the vehicle control group (Fig. 6a). In addition to pretreatment, results from time course experiments revealed that the infarct volume was also significantly reduced when CN was administered at 3, 4, and

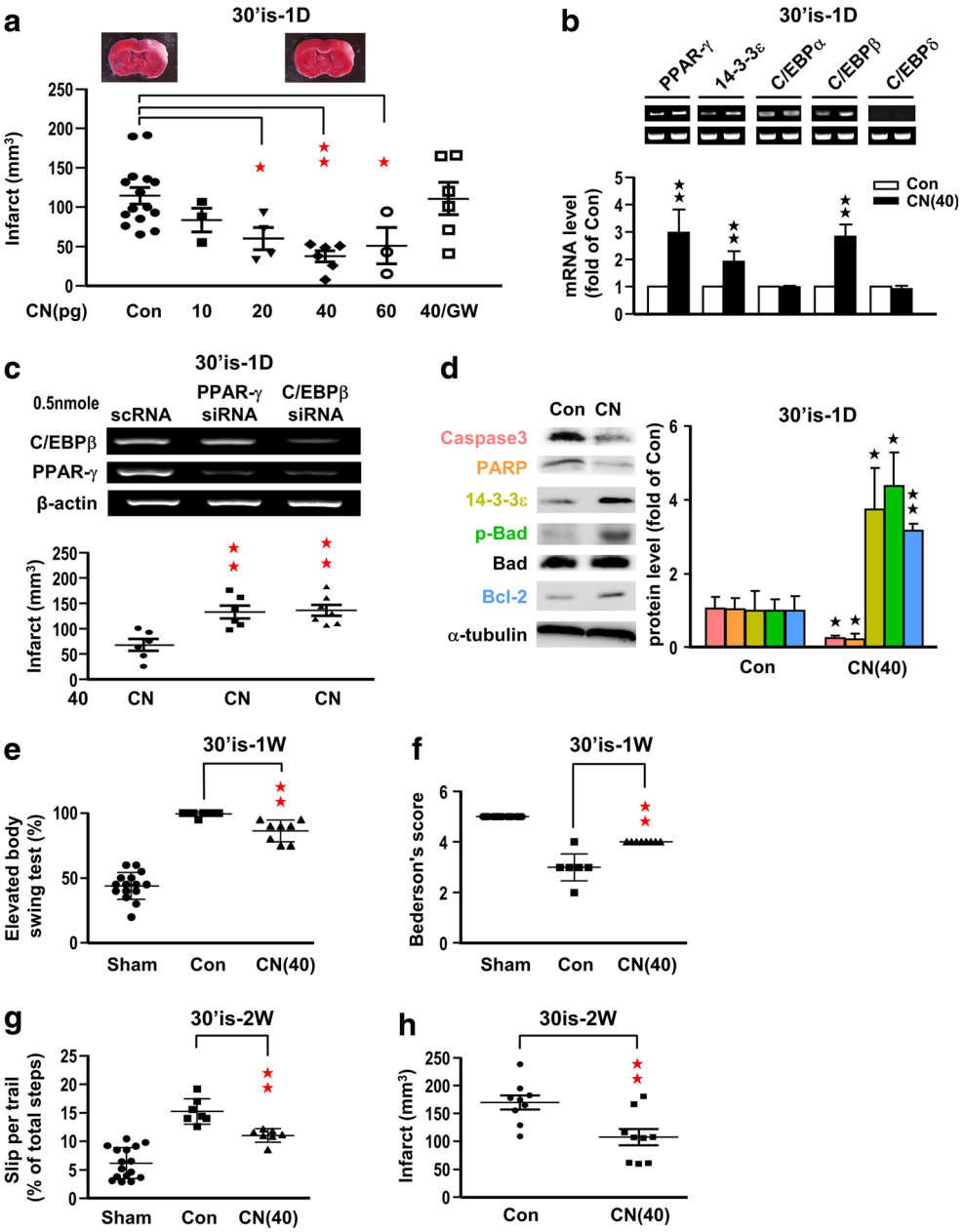

Fig. 5 *C. nutans* extract (CN) via upregulating PPAR-γ ameliorated ischemic brain injury and behavioral deficit. Immediately after 30-min MCA occlusion (30'is), rats were subjected to icv infusion of CN alone or together with GW9662 (165 ng), PPAR-γ siRNA, or C/EBPβ siRNA for infarct volume (**a**), mRNA levels (**b**), infarct volume (**c**), and protein levels (**d**) measurement at 24-h reperfusion (30'is-1D); or for behavior tests (**e**~**g**) and infarct volume (**h**) measurement at 1- or 2-week reperfusion (30'is-1/2 W). Sham refers to sham-operated control. Data are mean ± SD, $n \geq 6$. $^{\star}P < 0.05$ and $^{\star\star}P < 0.01$ versus vehicle control

6 h after 30-min MCA occlusion (Fig. 6b). However, CN was no longer effective in attenuating cerebral infarction when administered 24 h after 30-min MCA occlusion (Fig. 6b). Nonetheless, significant infarct volume reduction was also noted in the 24 h (1D) post-ischemic CN treatment group when ischemic severity was reduced to 15-min MCA occlusion (Fig. 6c). With the 15-min ischemia group, and based on Bederson's postural task, elevated body swing test, and the ladder rung walking test, CN administration also resulted in better functional outcomes as observed at 1-week (Fig. 6d, e) and 2-week (Fig. 6f, g) reperfusion. Finally, using the T2-weighted MRI images, smaller infarct volume was noted in the CN treated group at the 2 weeks after 15-min ischemia (Fig. 6h). The aforementioned results showed that CN is of clinical benefits to brain health.

Discussion

Although *C. nutans* has a long history for its diverse medicinal use to treat a number of remedies, whether this herb can be used to treat stroke damage has not been studied [10, 11]. In a previous study, we showed that pretreatment of CN could attenuate OGD-induced cell death in primary cortical neurons, astrocytes, and endothelial cells [14]. These results prompted us to consider the possibility that *C. nutans* might be useful for

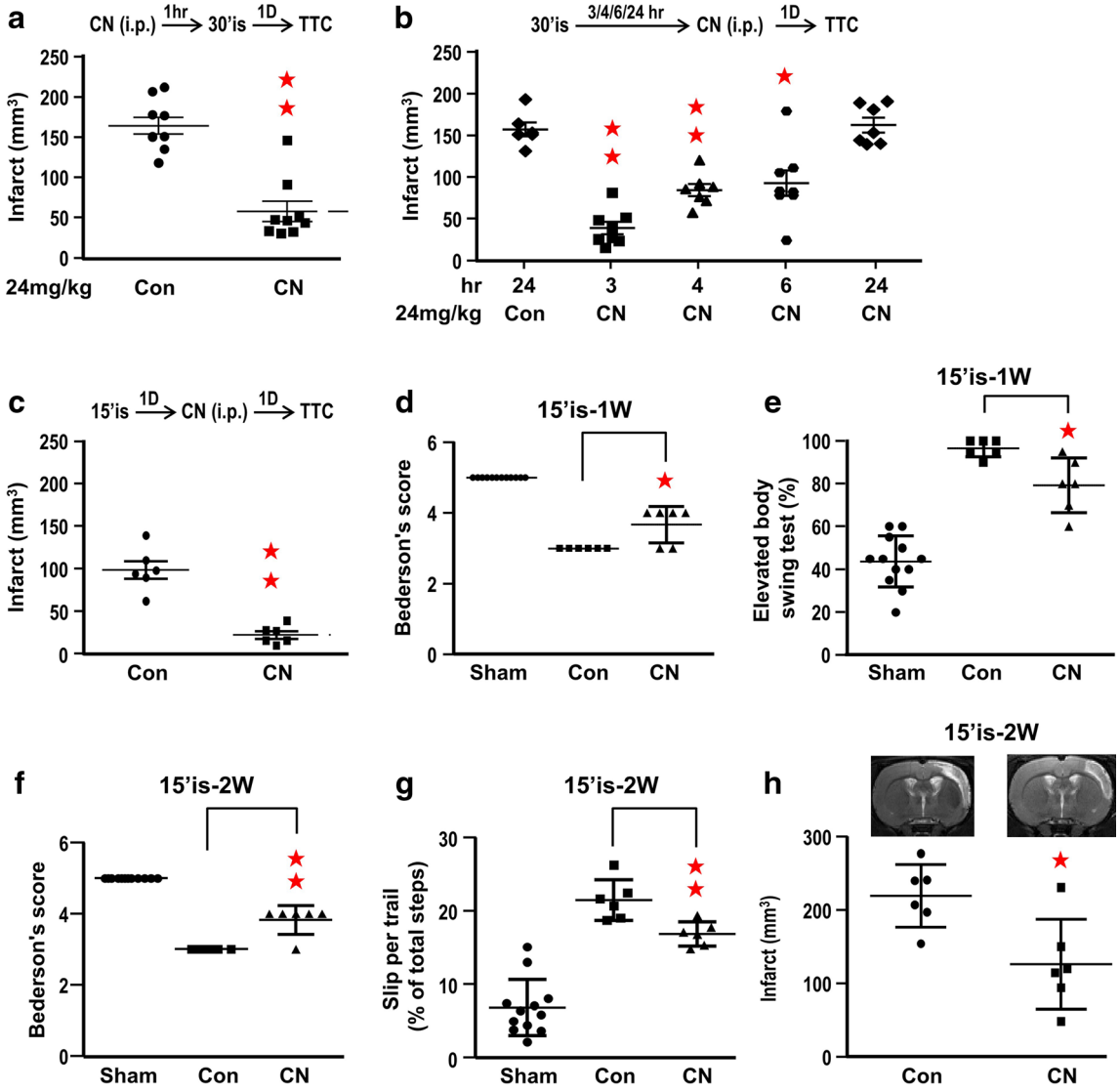

Fig. 6 Intraperitoneal (i.p.) injection of *C. nutans* extract (CN) improved post-ischemic brain damage and behavioral deficit. Rats were subjected to i.p. injection of CN at 1 h before or at 3, 4, 6, and 24 h after 30-min MCA occlusion (30'is; **a**, **b**). Or rats were subjected to i.p. injection of 24 mg/kg CN at 24 h after 15-min MCA occlusion (15'is; **c**~**h**). Infarct volume were determined 1D later by TTC (**a**~**c**) or 2 weeks later by MRI (**h**). Functional outcomes were assessed at 15'is-1 week (**d**, **e**) or 15'is-2 weeks (**f**, **g**). Sham refers to sham-operated control. Data are mean ± SD, $n \geq 6$. $^{\star}P < 0.05$ and $^{\star\star}P < 0.01$ versus vehicle control

mitigating stroke damage. In the present study, we demonstrated that CN reduced OGD-induced apoptotic neuronal death in a time- and concentration-dependent manner. Besides pretreatment, the protective effect of CN could be observed upon administration at the onset as well as immediately after hypoxia treatment.

The in vitro hypoxia findings were further translated to results obtained from in vivo ischemic model. A significant reduction in infarct volume was also observed upon i.p. injection of CN either at 1 h prior to 30-min MCA occlusion, or at 3, 4, and 6 h after 30-min MCA occlusion. In fact, when rats were subjected to a milder ischemic insult (i.e., 15-min MCA occlusion), a significant reduction of infarct volume could still be observed when CN was i.p. administered at 24 h after ischemia. In all protocols, the decrease in infarct volume due to CN administration was positively correlated with better functional recovery. Notably that in these experiments, all treatments were based on a single-dose administration; thus, multiple administrations might lead to even better outcomes. Although this study has not tested effects of oral administration of CN, it is reasonable that these other modes of administration will provide similar protective results. A recent study with animals indicated no observable adverse effects with oral doses of the extract up to 2000 mg/kg/day for 90 days [30]. To the best of our knowledge, we are probably the first to unveil the high prophylactic and therapeutic potency of *C. nutans* against ischemic stroke.

It is worth noting that 30% of ischemic stroke incidences are associated with the prevalence of infection (due to virus, bacterium, prion or fungus). Furthermore, the severity and clinical outcome of ischemic stroke are often worsened when preceded by infection [31, 32]. The frequency of post-stroke infection complication is also around 30%, which is independently associated with poorer functional outcome as compared with patients without post-stroke infection [33]. And patients with acute stroke had significantly better outcome when treated with minocycline, a tetracycline antibiotic [34]. Moreover, trials of antibiotics for the prevention of pre- and post-stroke infection have shown promising results in the improvement of outcome [31]. Coincidently, systematic review and meta-analysis of randomized clinical trials show anti-viral and anti-microbial effects of *C. nutans* extract in patients with herpes infection [10, 11, 35], which further strengthen the potential for *C. nutans* to offer prophylactic and therapeutic treatment for stroke, and greatly advocating the contention of using *C. nutans* as a nutraceutical for improvement of brain health as well as reduce risk for stroke.

Although *C. nutans* is endowed with anti-inflammatory, anti-viral, and anti-oxidant properties, information on cellular and molecular mechanisms underlying its mode of actions remains elusive [10, 11]. Here, we have linked the action of *C. nutans* to PPAR-γ (NR1C3 or glitazone receptor), a ligand-modulated transcription factor belonging to the nuclear hormone receptor superfamily [36]. Previously, we and others have demonstrated PPAR-γ as a therapeutic target for treating ischemic stroke, mainly due to its anti-inflammatory, anti-oxidant, and anti-apoptosis activities [18, 20, 22, 23, 37–41]. Considering that many biological activities of *C. nutans* overlap with those for PPAR-γ, there is strong rationale for a link between the two, especially with regard to actions on cerebral ischemia. An important initial finding is the effects of PPAR-γ antagonist GW9662 and PPAR-γ siRNA to neutralize the effects of *C. nutans* extract to attenuate hypoxia-induced apoptotic cell death. Reporter assay study further demonstrated that *C. nutans* extract not only increased PPAR-γ transcriptional activity but also increased 14-3-3ε transcription, a downstream gene of PPAR-γ known to bind phospho-Bad to inhibit apoptosis [22]. Taken together, these results strongly support the ability for *C. nutans* extract to protect hypoxia-induced apoptotic neuronal death, in a large part, by promoting the PPAR-γ → 14-3-3ε signal cascade.

This study also unveiled a unique C/EBP binding site (-332~-325) at the 5′-region of PPAR-γ promoter which is responsible for enhancing PPAR-γ transcription by CN. Albeit the presence of six C/EBP isoforms [42, 43], only C/EBPβ expression was upregulated by CN. Results of reporter and ChIP assays further demonstrated that CN could enhance binding of C/EBPβ to this C/EBP binding site, and subsequently augment PPAR-γ transcription. In both in vitro and in vivo protocols, downregulation either C/EBPβ or PPAR-γ by siRNA could offset the neuroprotective effect of CN. Although it is well established in adipocytes that C/EBPβ plays an essential role in adipogenesis by transactivating the expression of PPAR-γ [42]. In the present study, we clearly demonstrated that C/EBPβ by binding to PPAR-γ promoter directly triggered the expression of PPAR-γ. To the best of our knowledge, we are probably the first to report this novel transcriptional regulation in neuron.

In summary, this study unveiled the prophylactic and therapeutic effects of *C. nutans* against ischemic stroke through promoting the C/EBPβ-driven PPAR-γ transcription. Recognition of *C. nutans* extract to exert neuroprotective effects through the anti-apoptotic C/EBPβ → PPAR-γ → 14-3-3ε pathway not only provides novel therapeutic targets but also paves new ways for potential drug candidates for prevention and treatment of ischemic stroke. Since a number of neurodegenerative diseases also involve oxidative/inflammatory damage, future studies can be extended to test ability of this herbal medicine and its active components to ameliorate other neurological disorders.

Acknowledgements We thank the Taiwan Mouse Clinic (TMC; http://tmc.sinica.edu.tw/index.html; MRI: Yu-Ying Tung) for technical support. All authors have read and agreed to the manuscript as written.

Funding Information This work was supported by grants from the Minister of Science and Technology and Academia Sinica of Taiwan to T.N. Lin.

Compliance with Ethical Standards

Conflict of Interest The authors declare that they have no conflict of interest.

References

1. Writing Group Members, Mozaffarian D, Benjamin EJ, Go AS, Arnett DK, Blaha MJ, Cushman M, Das SR et al, American Heart Association Statistics Committee; Stroke Statistics Subcommittee (2016) Heart disease and stroke statistics—2016 update: a report from the American Heart Association. Circulation 133(4):e38–360
2. Moskowitz MA, Lo EH, Iadecola C (2010) The science of stroke: mechanisms in search of treatments. Neuron 67(2):181–198
3. National Institute of Neurological Disorders and Stroke rt-PA Stroke Study Group (1995) Tissue plasminogen activator for acute ischemic stroke. N Engl J Med 333(24):1581–1587
4. Wang X, Lee SR, Arai K, Lee SR, Tsuji K, Rebeck GW, Lo EH (2003) Lipoprotein receptor-mediated induction of matrix metalloproteinase by tissue plasminogen activator. Nat Med 9(10):1313–1317
5. Chen YC, Wu JS, Yang ST, Huang CY, Chang C, Sun GY, Lin TN (2012) Stroke, angiogenesis and phytochemicals. Front Biosci (Schol Ed) 4:599–610
6. Goetz ME, Judd SE, Hartman TJ, McClellan W, Anderson A, Vaccarino V (2016) Flavanone intake is inversely associated with risk of incident ischemic stroke in the REasons for Geographic and Racial Differences in Stroke (REGARDS) Study. J Nutr 146(11):2233–2243

7. Kim J, Fann DY, Seet RC, Jo DG, Mattson MP, Arumugam TV (2016) Phytochemicals in ischemic stroke. NeuroMolecular Med 18(3):283–305
8. Lee J, Jo DG, Park D, Chung HY, Mattson MP (2014) Adaptive cellular stress pathways as therapeutic targets of dietary phytochemicals: focus on the nervous system. Pharmacol Rev 66(3):815–868
9. Sun AY, Wang Q, Simonyi A, Sun GY (2008) Botanical phenolics and brain health. NeuroMolecular Med 10(4):259–274
10. Alam A, Ferdosh S, Ghafoor K, Hakim A, Juraimi AS, Khatib A, Sarker ZI (2016) Clinacanthus nutans: a review of the medicinal uses, pharmacology and phytochemistry. Asian Pac J Trop Med 9(4):402–409
11. Zulkipli IN, Rajabalaya R, Idris A, Sulaiman NA, David SR (2017) Clinacanthus nutans: a review on ethnomedicinal uses, chemical constituents and pharmacological properties. Pharm Biol 55(1): 1093–1113
12. Ng PY, Chye SM, Ng CH, Koh RY, Tiong YL, Pui LP, Tan YH, Lim CS et al (2017) Clinacanthus nutans hexane extracts induce apoptosis through a caspase-dependent pathway in human cancer cell lines. Asian Pac J Cancer Prev 18(4):917–926
13. Tan CS, Ho CF, Heng SS, Wu JS, Tan BK, Ng YK, Sun GY, Lin TN et al (2016) *Clinacanthus nutans* extracts modulate epigenetic link to cytosolic phospholipase A_2 expression in SH-SY5Y cells and primary neurons. NeuroMolecular Med 18(3):441–452
14. Tsai HD, Wu JS, Kao MH, Chen JJ, Sun GY, Ong WY, Lin TN (2016) *Clinacanthus nutans* protects cortical neurons against hypoxia-induced toxicity by downregulating HDAC1/6. NeuroMolecular Med 18(3):274–282
15. Lee JE, Ge K (2014) Transcriptional and epigenetic regulation of PPAR-γ expression during adipogenesis. Cell Biosci 4:29
16. Schweizer S, Meisel A, Märschenz S (2013) Epigenetic mechanisms in cerebral ischemia. J Cereb Blood Flow Metab 33(9): 1335–1346
17. Goldberg MP, Choi DW (1993) Combined oxygen and glucose deprivation in cortical cell culture: calcium-dependent and calcium-independent mechanisms of neuronal injury. J Neurosci 13(8):3510–3524
18. Wu JS, Tsai HD, Cheung WM, Hsu CY, Lin TN (2016) PPAR-γ ameliorates neuronal apoptosis and ischemic brain injury via suppressing NF-κB-driven p22phox transcription. Mol Neurobiol 53(6):3626–3645
19. Huang CY, Chen JJ, Wu JS, Tsai HD, Lin H, Yan YT, Hsu CY, Ho YS et al (2015) Novel link of anti-apoptotic ATF3 with pro-apoptotic CTMP in the ischemic brain. Mol Neurobiol 51(2):543–557
20. Wu JS, Lin TN, Wu KK (2009) Rosiglitazone and PPAR-γ overexpression protect mitochondrial membrane and prevent mitochondria-mediated apoptosis by upregulating anti-apoptotic Bcl-2 family proteins. J Cell Physiol 220(1):58–71
21. Lin TN, Wang CK, Cheung WM, Hsu CY (2000) Induction of angiopoietin and tie receptor mRNA expression following cerebral ischemia-reperfusion. J Cereb Blood Flow Metab 20:387–395
22. Wu JS, Cheung WM, Tsai YS, Chen YT, Fong WH, Tsai HD, Chen YC, Liou JY et al (2009) Ligand-activated PPAR-γ protects against ischemic cerebral infarction and neuronal apoptosis by 14-3-3ε upregulation. Circulation 119(8):1124–1134
23. Wu JS, Tsai HD, Huang CY, Chen JJ, Lin TN (2014) 15-deoxy-$\Delta^{12,14}$-PGJ_2 via activating peroxisome proliferator-activated receptor-gamma suppresses p22phox transcription to protect brain endothelial cells against hypoxia-induced apoptosis. Mol Neurobiol 50(1): 221–238
24. Lin TN, He YY, Wu G, Khan M, Hsu CY (1993) Effect of brain edema on infarct volume in a focal cerebral ischemia model in the rat. Stroke 24:117–121
25. Lin H, Lin TN, Cheung WM, Nian GM, Tseng PH, Chen SF, Chen JJ, Shyue SK et al (2002) Cyclooxygenase-1 (COX-1) and bicistronic COX-1/prostacyclin synthase gene transfer protect against ischemic cerebral infarction. Circulation 105:1962–1969
26. Bederson JB, Pitts LH, Tsuji M, Nishimura MC, Davis RL, Bartkowski H (1986) Rat middle cerebral artery occlusion: evaluation of the model and development of a neurologic examination. Stroke 17:472–476
27. Borlongan CV, Cahill DW, Sanberg PR (1995) Locomotor and passive avoidance deficits following occlusion of the middle cerebral artery. Physiol Behav 58(5):909–917
28. Metz GA, Whishaw IQ (2002) Cortical and subcortical lesions impair skilled walking in the ladder rung walking test: a new task to evaluate fore- and hindlimb stepping, placing, and co-ordination. J Neurosci Methods 115(2):169–179
29. Lin TN, Sun SW, Cheung WM, Li F, Chang C (2002) Dynamic changes in cerebral blood flow and angiogenesis after transient focal cerebral ischemia in rats: evaluation with serial MRI. Stroke 33:2985–2991
30. Farsi E, Esmailli K, Shafaei A, Moradi Khaniabadi P, Al Hindi B, Khadeer Ahamed MB, Sandai D, Abdul Sattar M et al (2016) Mutagenicity and preclinical safety assessment of the aqueous extract of Clinacanthus nutans leaves. Drug Chem Toxicol 39(4):461–473
31. Emsley HC, Hopkins SJ (2008) Acute ischaemic stroke and infection: recent and emerging concepts. Lancet Neurol 7(4):341–353
32. Ionita CC, Siddiqui AH, Levy EI, Hopkins LN, Snyder KV, Gibbons KJ (2011) Acute ischemic stroke and infections. J Stroke Cerebrovasc Dis 20(1):1–9
33. Westendorp WF, Nederkoorn PJ, Vermeij JD, Dijkgraaf MG, van de Beek D (2011) Post-stroke infection: a systematic review and meta-analysis. BMC Neurol 11:110
34. Lampl Y, Boaz M, Gilad R, Lorberboym M, Dabby R, Rapoport A, Anca-Hershkowitz M, Sadeh M (2007) Minocycline treatment in acute stroke: an open-label, evaluator-blinded study. Neurology 69(14):1404–1410
35. Kongkaew C, Chaiyakunapruk N (2011) Efficacy of Clinacanthus nutans extracts in patients with herpes infection: systematic review and meta-analysis of randomised clinical trials. Complement Ther Med 19(1):47–53
36. Michalik L, Auwerx J, Berger JP, Chatterjee VK, Glass CK, Gonzalez FJ, Grimaldi PA, Kadowaki T et al (2006) International Union of Pharmacology. LXI. Peroxisome proliferator-activated receptors. Pharmacol Rev 58(4):726–741
37. Chen YC, Wu JS, Tsai HD, Huang CY, Chen JJ, Sun GY, Lin TN (2012) Peroxisome proliferator-activated receptor gamma (PPAR-γ) and neurodegenerative disorders. Mol Neurobiol 46(1):114–124
38. Collino M, Patel NS, Thiemermann C (2008) PPARs as new therapeutic targets for the treatment of cerebral ischemia/reperfusion injury. Ther Adv Cardiovasc Dis 2(3):179–197
39. Fong WH, Tsai HD, Chen YC, Wu JS, Lin TN (2010) Anti-apoptotic actions of PPAR-γ against ischemic stroke. Mol Neurobiol 41(2–3):180–186
40. Lin TN, Cheung WM, Wu JS, Chen JJ, Lin H, Chen JJ, Liou JY, Shyue SK et al (2006) 15d-Prostaglandin J_2 protects brain from ischemia-reperfusion injury. Arterioscler Thromb Vasc Biol 26: 481–487
41. Villacorta L, Schopfer FJ, Zhang J, Freeman BA, Chen YE (2009) PPARgamma and its ligands: therapeutic implications in cardiovascular disease. Clin Sci (Lond) 116(3):205–218
42. Guo L, Li X, Tang QQ (2015) Transcriptional regulation of adipocyte differentiation: a central role for CCAAT/enhancer-binding protein (C/EBP) β. J Biol Chem 290(2):755–761
43. Tsukada J, Yoshida Y, Kominato Y, Auron PE (2011) The CCAAT/enhancer (C/EBP) family of basic-leucine zipper (bZIP) transcription factors is a multifaceted highly-regulated system for gene regulation. Cytokine 54(1):6–19